Pergamon

PII: S0191-8141(97)00095-3

Journal of Structural Geology, Vol. 20, No. 4, pp. 339 to 353, 1998

0191-8141/98 $19.00 + 0.00

Map-view interference of monoclinal folds

ENRIQUE NOVOA

Departamento de Ciencias de la Tierra, Gerencia de Exploración y Producción, INTEVEP, Los Teques Estado Miranda, Venezuela

VAN MOUNT

ARCO Exploration and Production Technology, 2300 W. Plano Parkway Plano, Texas 75075, U.S.A.

and

JOHN SUPPE

Department of Geosciences, Princeton University Princeton, New Jersey 08544, U.S.A.

(*Received* 1 *February* 1996; *accepted in revised form* 12 *September* 1997)

Abstract—Outcrop observations and laboratory experiments show that many small chevron folds form by interference of monoclinal kink bands in multilayer buckling. Kink-band interference has also been proposed for some map-scale folds. Furthermore, fault-related folding provides additional mechanisms of monoclinal fold generation, other than buckling, and thus makes kink-band interference all the more conceptually plausible as a significant large-scale process. In this paper we document several relatively simple examples of map-scale monoclinal fold interference, including three interfering monoclines of the Colorado Plateau, a seismically-imaged example in the Perdido foldbelt of the Gulf of Mexico, and a more complex example from seismic mapping in the Santa Barbara Channel, California. Kink-band interference has normally been analyzed in cross section. Here we emphasize the map-view phenomena and present a simple balanced three-dimensional model of the interference geometry, treating the monoclines as two independent kink bands, which does not depend of the kink-band folding mechanism. This model predicts the shape of the jog produced by crossing monoclines and is used to help evaluate the role of interference in the map-view geometry of our examples. The documentation of these simple examples supports the concept that more complex monoclinal fold interference could be a significant phenomenon in the upper crust. © 1998 Elsevier Science Ltd. All rights reserved

INTRODUCTION

Chevron folds and other complex fold geometries can form by the complex interference of monoclinal kink bands (e.g. Paterson and Weiss, 1966; Weiss, 1968; Honea and Johnson, 1976; Stewart and Alvarez, 1991). This has been demonstrated from outcrop observations and laboratory experiments on slate, phyllites and analog materials such as paper cards and rubber strips. The same interference process has also been proposed for the origin of some map-scale compressive folds (e.g. the Appalachian foldbelt: Faill, 1969, 1973; Cantabrian foldbelt: Julivert and Marcos, 1973; Stewart, 1993; Alvarez-Marron, 1995). Thus large-scale fold interference is probably a common process in the upper crust.

This possibility of important map-scale fold interference is made all the more plausible by the recognized importance of fault-related folding in the upper crust. The various proposed and demonstrated fault-related folding mechanisms provide a number of ways to generate large-scale monoclinal fold limbs, involving both kink-band migration and limb rotation (e.g. Erslev, 1991; Hardy and Poblet, 1994; Jamison, 1987; Mitra, 1990; Narr and Suppe, 1994; Suppe, 1983, 1985; Suppe and Medwedeff, 1990; Wickham, 1995; Xiao and Suppe, 1992). Furthermore, balanced forward modeling of multibend compressive fault-bend folding by Medwedeff and Suppe (1997) shows that even with relatively small numbers of fault bends, immensely complex fold interference patterns are predicted solely from the application of the simple fault-bend folding assumptions of conservation of bed length and layer thickness.

Therefore map-scale fold interference in the upper crust seems likely, but in many cases could be too complex to image or decipher in cross section from reflection seismic profiles and surface geologic data. In this paper we document five examples of map-scale interference of monoclinal folds: three exposed in the Colorado Plateau and two offshore seismic examples from the Perdido Fold Belt in the Gulf of Mexico and the Santa Barbara Channel in southern California.

Previous studies of monoclinal fold interference have focused largely on analysis in cross section of kink-band interference resulting from multilayer buckling, where quite complex phenomena are observed in the field and laboratory (e.g. Paterson and Weiss, 1966; Weiss, 1968; Honea and Johnson, 1976; Stewart and Alvarez, 1991). As we move to map-scale structures, fault-related folding provides additional processes of monocline formation. Therefore we begin with a brief consideration of the

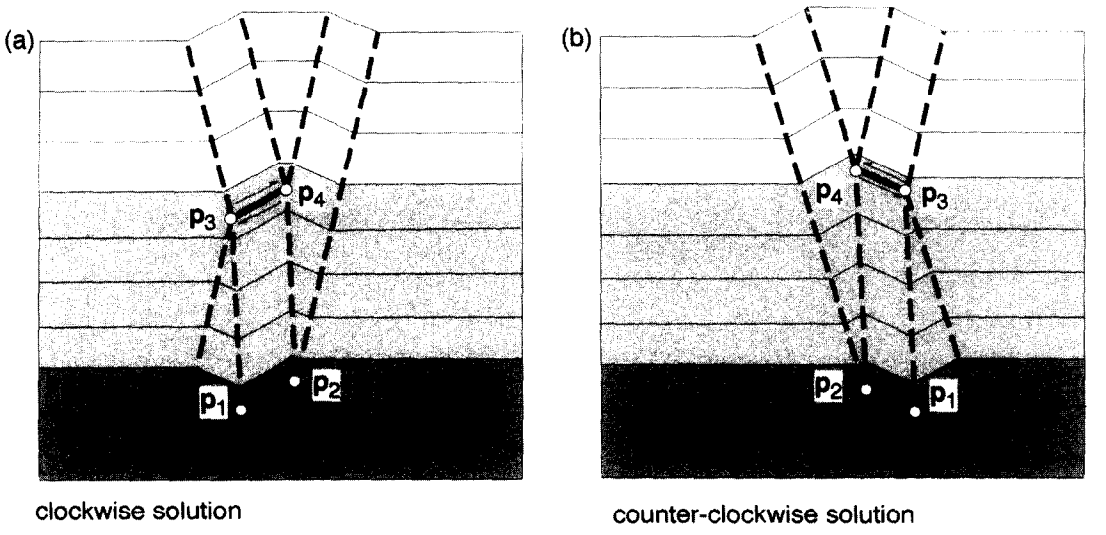

Fig. 1. Two possible balanced solutions for the interference of opposing kink bands in cross-section view. (a) In the clockwise interference solution the through-going kink band is sheared in a clockwise sense whereas the other kink band exists in two fragments linked by the bedding surfaces containing axial-surface branch points of opposite sign. (b) In the counter-clockwise interference solution the through-going kink band is sheared in a counter-clockwise sense. The axial surfaces of the fragmented kink band are linked by a bedding-parallel slip surface. Note that the sense of rotation depends on the viewing direction.

simple interference in cross section of two intersecting monoclinal kink bands generated by various fault-related fold models. We then develop a simple geometrical model of three-dimensional interference of two independent monoclinal kink bands, which does not assume a folding mechanism. This three-dimensional model is then used to help analyze the field examples in map view.

SIMPLE INTERFERENCE OF FAULT-RELATED FOLDS IN CROSS SECTION

A basic principle of many fault-related fold theories is that folds are created by slip past fault bends and through termination of slip at fault tips. Fault-related folding mechanisms that generate folds, either through kink-band migration or limb rotation, include a variety of fault-bend folding mechanisms (Apotria *et al.*, 1992; Mitra, 1990; Narr and Suppe, 1994; Shaw *et al.*, 1994; Suppe, 1983; Xiao and Suppe, 1992) and various tip-line folding mechanisms, including fault propagation folding (Suppe, 1985; Suppe and Medwedeff, 1990), trishear folding (Erslev, 1991; Hardy and Ford, 1997), displacement-gradient folding (Wickham, 1995) and wedge tips (Medwedeff, 1992; Narr and Suppe, 1994). Furthermore, given faults with multiple bends and closely spaced faults, it is expected that monoclinal folds generated at different fault bends or fault tips will in some instances intersect and interfere with one another.

Simple interference

Observation of small-scale interference of kink bands shows immense complexity that is not understood in detail. Here we consider interference of the simplest possible sort, simple crossing of two antithetic monoclinal kink bands (Fig. 1). This geometry, as well as more complex ones, is discussed in detail by Medwedeff and Suppe (1997). Here we simply note that in cross section there are two possible balanced solutions that conserve layer thickness and bed length, given no shear. Figure 1(a) shows the clockwise solution, in which the through-going kink band is sheared in a clockwise sense. Figure 1(b) shows the counter-clockwise solution. Clockwise and counter-clockwise are of course relative to the direction of view. In both cases the one kink band is fragmented into two parts on either side of a sheared kink band. Axial surface branch points occur as opposite-sign pairs on the same horizon because of the requirement of conservation of shear in classical balancing (Suppe, 1983; Medwedeff and Suppe, 1997). The two interference solutions are of course just geometric possibilities; what actually happens in the rock depends on the history and mechanics of the deformation. For example if the kink bands form sequentially, the first formed band will be the sheared kink band.

Fault-related fold interference

Many structural scenarios can be envisaged to produce the simple kink-band interference shown in Fig. 1. To emphasize the possibility of fault-related folding, in addition to buckling mechanisms, we present seven fault-related fold scenarios in Fig. 2, each developed using a different fault-related folding mechanism or fault geometry.

Figure 2(a–c) were developed using fault-bend folding and show the interaction of kink bands which originated

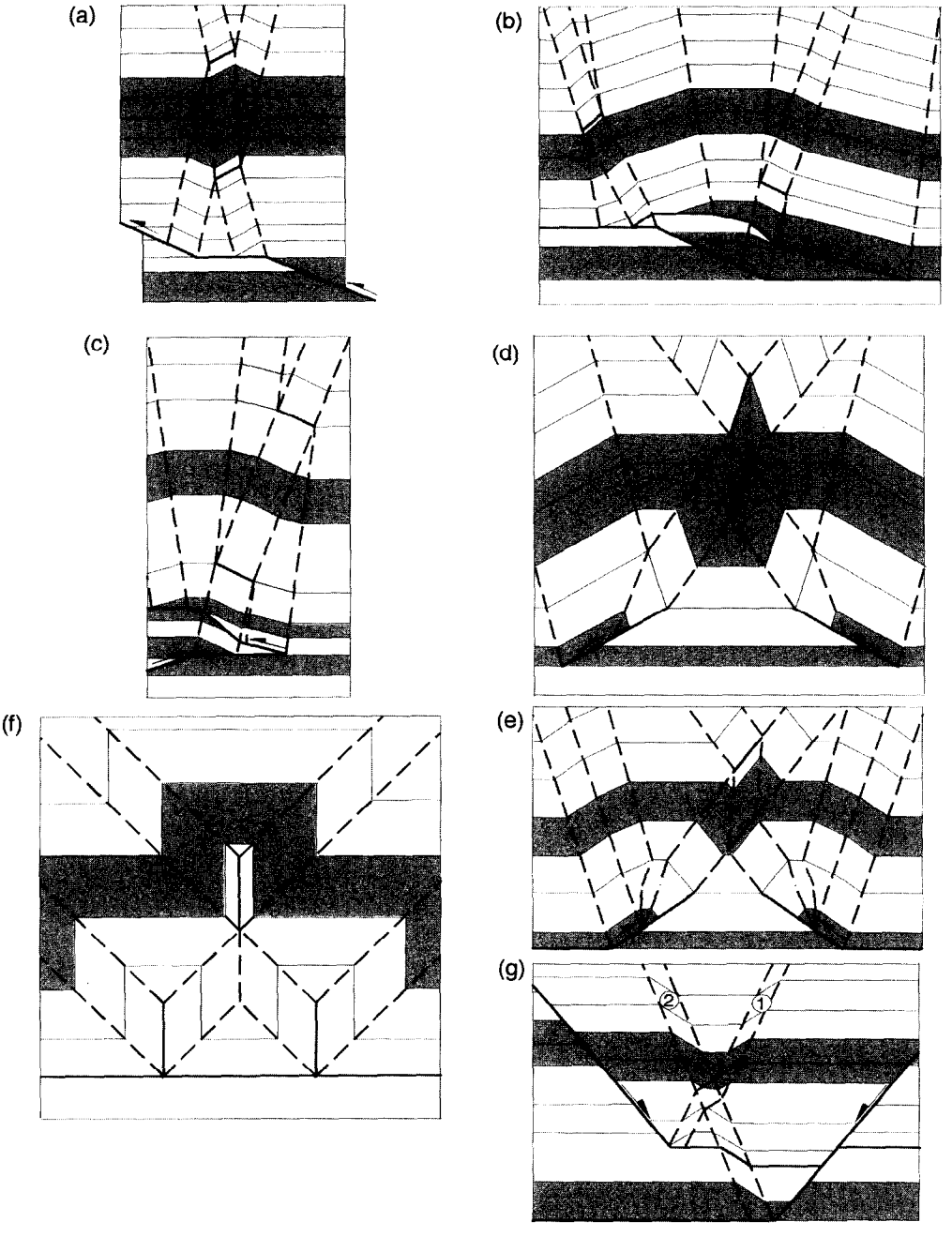

Fig. 2. Kink-band intersection may be envisaged for a number of folding mechanisms, including the following fault-related folding scenarios. (a) Kink bands developed on a ramp–flat–ramp fault interfere in a clockwise interference structure. (b) Imbrication of thrust faults may also generate interference structures. This case shows the interaction between the kink bands on front limbs and kink bands on back limbs related to each of the two faults. (c) Kink bands developed over a wedge structure interact with each other to form a clockwise interference structure. (d), (e) The interactions occur between the kink bands on the front limb of folds which were developed above two oppositely verging faults. In (d), the folds are fault-propagation folds. In (e), the folds are fault displacement-gradient folds. In both cases, a tight anticline-over-syncline structures are developed. (f) Kink bands of box folds which are closely spaced may interact and form interference structures. (g) Interference of folds as envisaged in an extensional environment. Kink band 1 which is the older one is sheared by kink band 2.

over bends in simple thrust faults. In Fig. 2(a) the kink bands are developed over a ramp–flat–ramp fault system producing a clockwise interference structure. In Fig. 2(b) the interference is developed over imbricated thrust faults. In the case of the back limb the younger kink band is generated externally to the older, similar to previous models. In contrast the new kink band on the front limb is generated internally to the old kink band and thus develops only half of the simple interference geometry. The interference on the front limb is counter clockwise whereas the interference on the back limb is clockwise. In Fig. 2(c) the interaction is related to a wedge structure producing a clockwise interference structure. Figure 2(g) shows a normal fault interference structure.

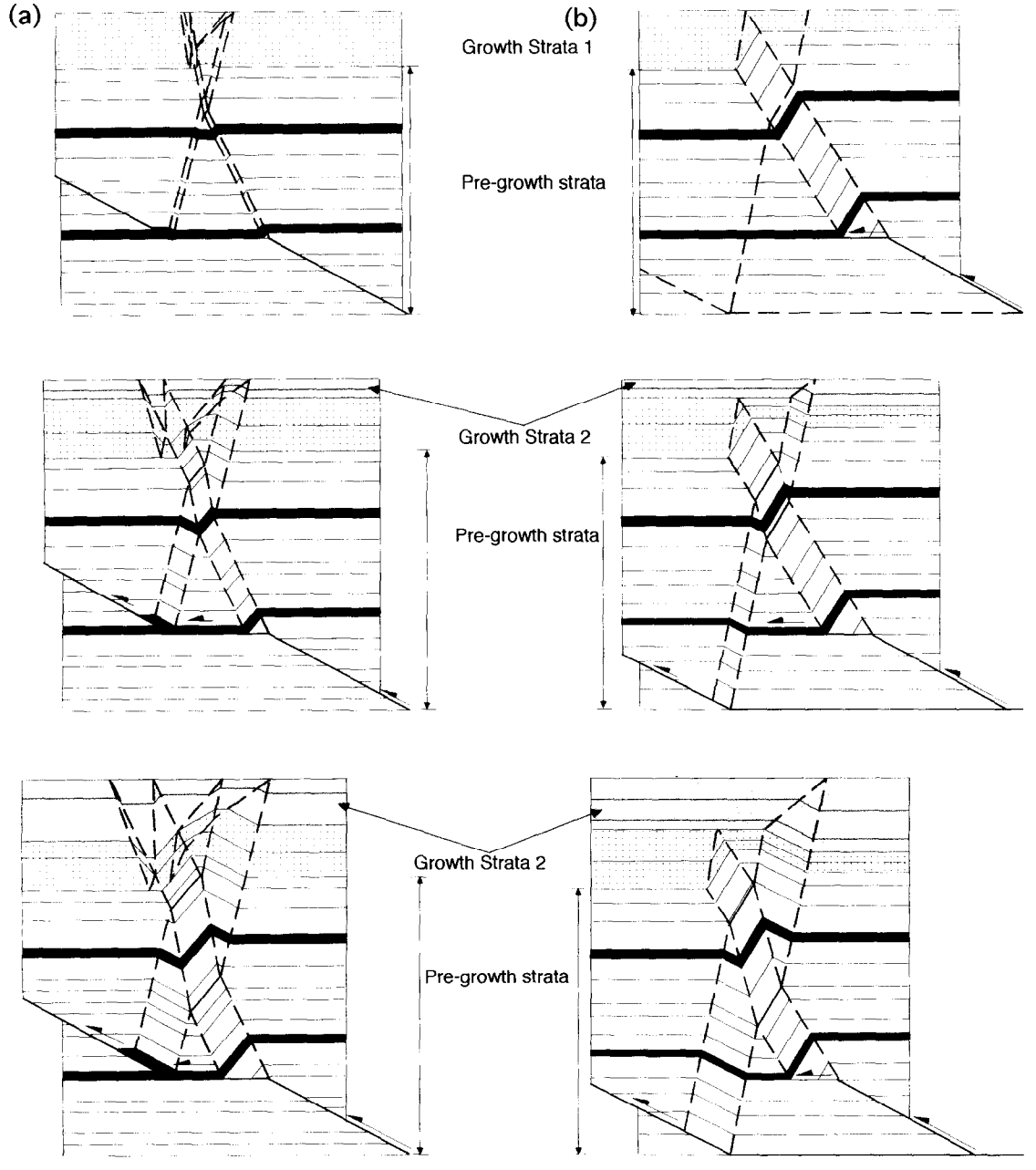

Fig. 3. Two kink-band interferences are developed with growth strata constraining kinematic histories. Note that the final fold shape is identical within the pre-growth strata above the faults, whereas the geometry of the growth strata is different, reflecting the kinematic path. In case (a), the interference occurs above an active ramp–flat–ramp geometry on a single fault. Thus the two kink bands develop simultaneously. In case (b), the two interfering kink bands are generated sequentially above faults of different ages. Considering the growth strata, in model (a) all four axial surfaces above the interference are active because both kink bands are growing simultaneously; therefore, all four axial surfaces generate growth triangles. In the sequential model (b) just one axial surface is active above the interference, which is linked to the active fault bend. Therefore, two growth triangles are developed sequentially, recording the times of activity of each kink band.

Other fault-bend fold interference geometries are presented by Narr and Suppe (1994) and Medwedeff and Suppe (1997).

Figure 2(d–f) shows several of the possible tip-line interference geometries. Figure 2(d & e) shows the interaction between the front limbs of two oppositely facing fault propagation and displacement-gradient folds. The result is a tight anticline-over-syncline structure, with clockwise interference. A degenerate case in which kink bands related to box folds interfere is shown in Fig. 2(f). A possible example of interfering head-to-head tip-line folds is Painter Reservoir, Wyoming (Lamerson, 1982).

Kinematic history

Some of the scenarios in Fig. 2 involve simultaneous formation of both kink bands by slip on a single fault

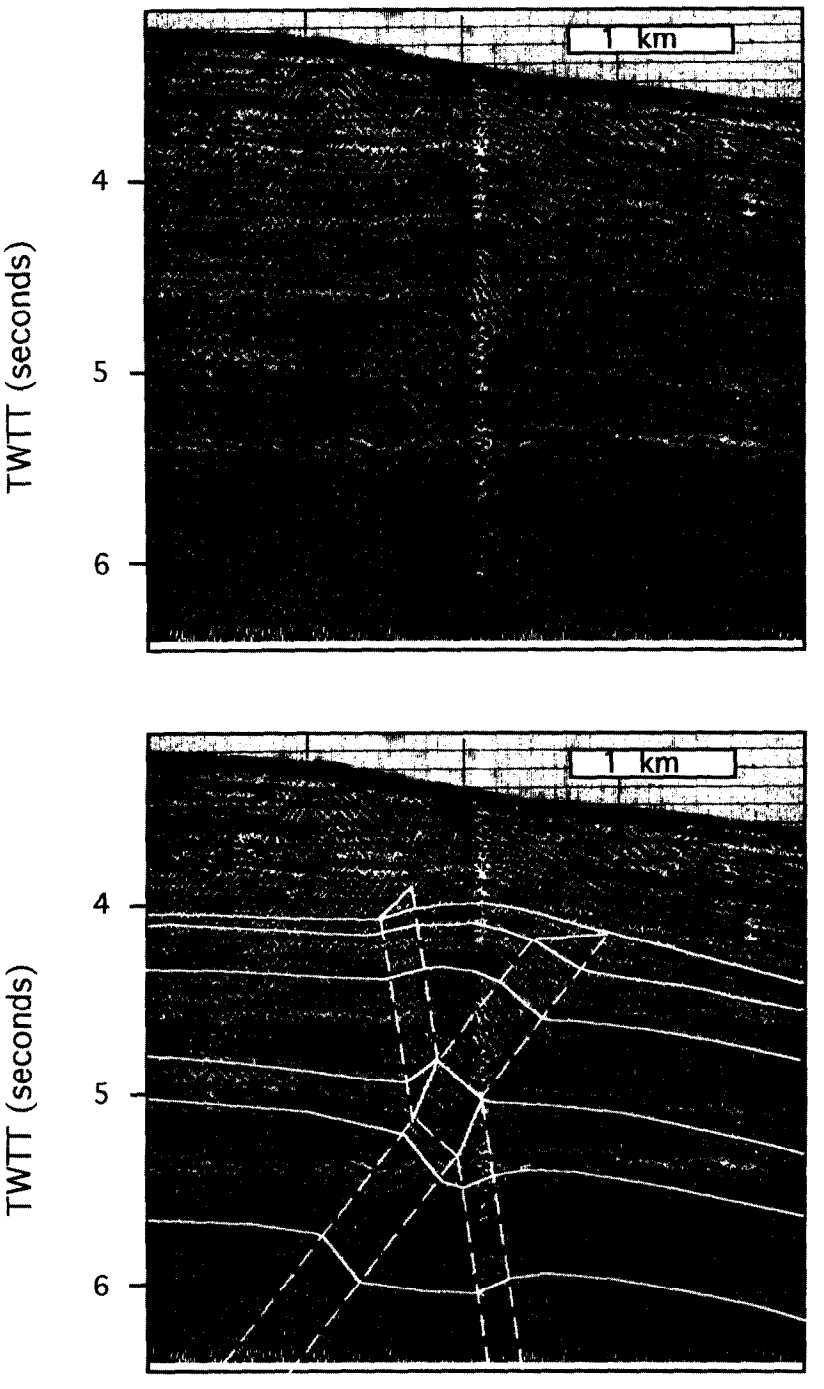

Fig. 4. Seismic image of kink band interference structure from the Perdido foldbelt, offshore Texas, Gulf of Mexico (Mount, 1989), showing a shape close to the theoretical counter-clockwise geometry (cf. Fig. 1b). The shape of the structure in the growth strata shows that the two kink bands are of different ages (cf. Fig. 3b). The older kink band stopped growing about the same time that the younger kink band began to form. See also Figs 9, 10 and 11. Seismic line provided by Texaco.

(Fig. 2 a & c). Medwedeff and Suppe (1997) present models of complex simultaneous kink-band growth and interference. Other scenarios involve sequential interference of kink bands formed at different times (e.g. Fig. 2 b & g). Still other scenarios could be either sequential or simultaneous (Fig. 2 d–f). In the case of Fig. 2(d & e), the left fault would be younger in the sequential case, because its fold shears the kink band of the right-hand fault.

The kinematic history of folding sometimes can be recorded in syntectonic growth strata (Suppe *et al.*, 1992), as shown in the two models of Fig. 3. Note that the two models have similar fold-interference geometry in the pre-growth strata and have the same total thickness of growth strata. The different geometries of the growth strata show that they have different kinematic histories. In Fig. 3(a) both kink bands are generated simulta-

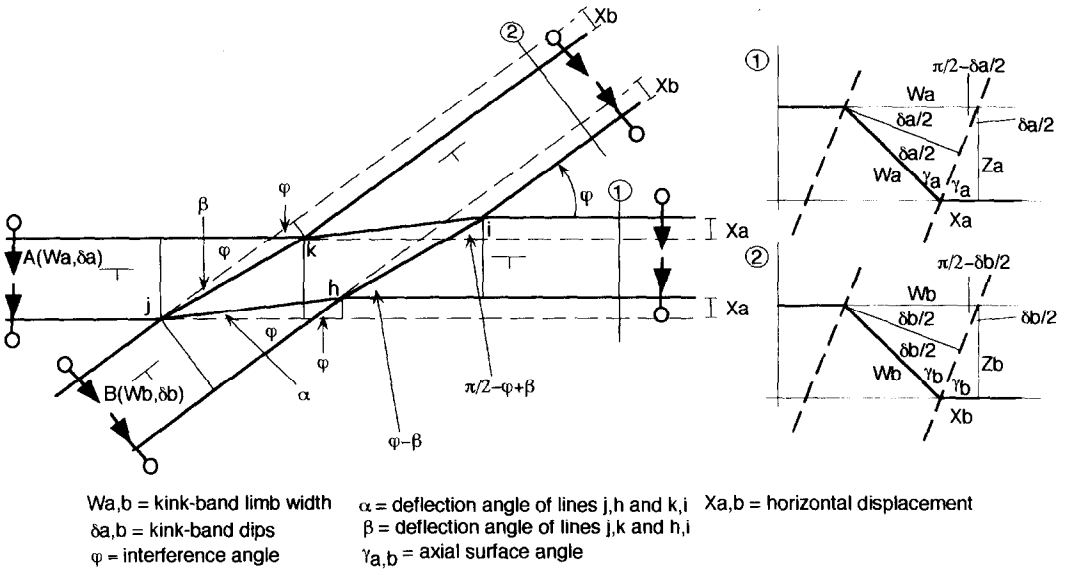

Fig. 5. Interference of two kink bands in plan view showing the angular relationships used in deriving the equations which describe interference geometry in map view. Angular relations are for a single stratigraphic horizon projected onto a horizontal datum.

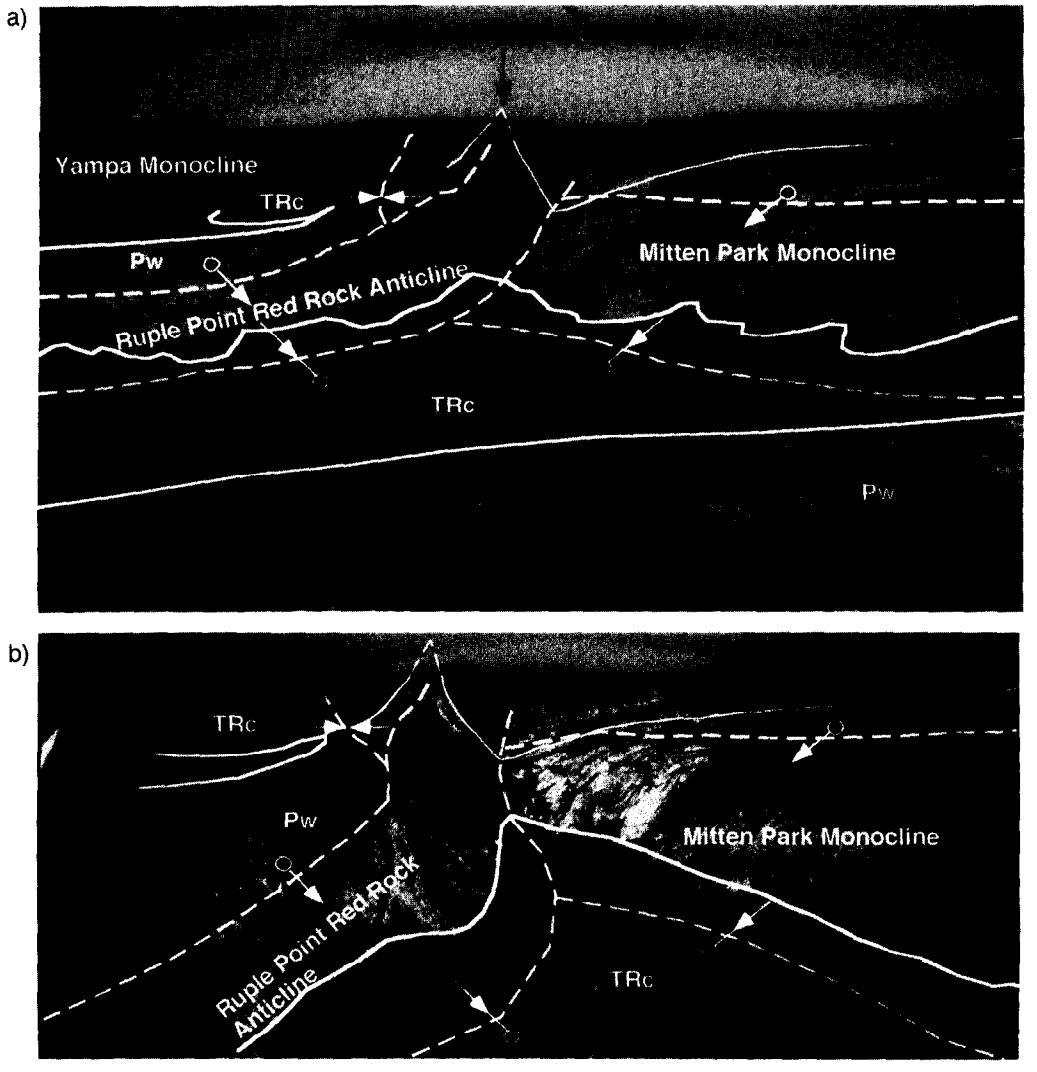

Fig. 6. Photographs of the Teepee interference structure looking west, Dinosaur National Monument, Utah. (a) Panoramic photo of the intersection between the Mitten Park monocline (on the right) and the Ruple Point–Red Rock Anticline (on the left). (b) Close up of the Teepee interference structure. Pw = Weber Sandstone, TRc = Chinle Formation.

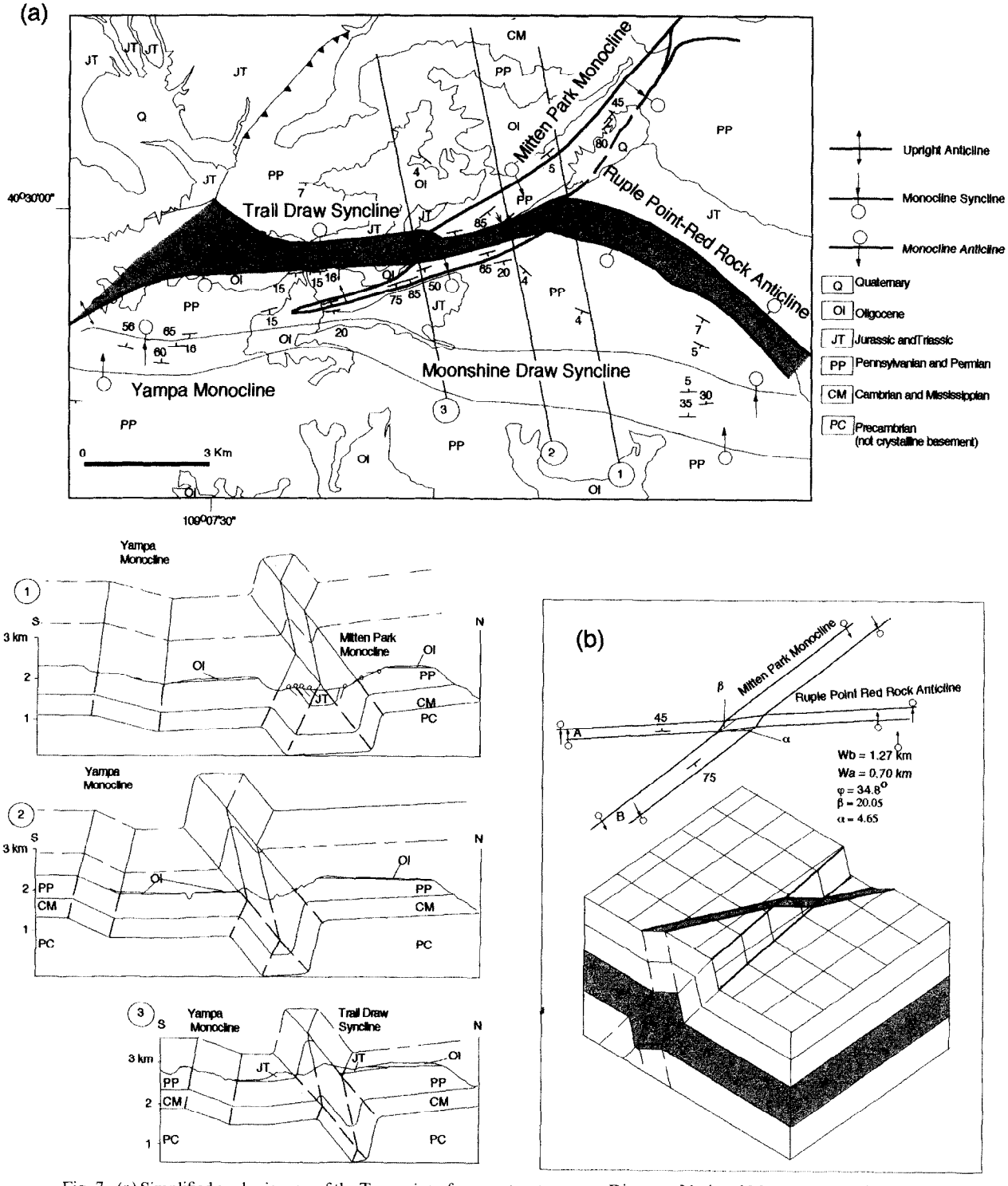

Fig. 7. (a) Simplified geologic map of the Teepee interference structure area, Dinosaur National Monument, Utah (Hansen *et al.*, 1983). Three cross sections illustrate the interference between the Mitten Park monocline and the Ruple Point–Red Rock anticline. This interaction forms a clockwise anticline-over-syncline structure when viewed from the west. In order to illustrate the interference in cross section, we have defined the rounded fold hinges by a unique bisecting axial surface. Notice that we have not interpreted any structure in the Precambrian basement (Uinta Mountain Group), for lack of constraints. (b) Plan view and three dimensional model of the Teepee structure.

neously by displacement on a single fault. In contrast, Fig. 3(b) shows sequential development by sequential slip on two faults (note that the fold geometry in Fig. 3a could be generated by simultaneous slip on the two faults of Fig. 3b).

Figure 4 shows a detail of a seismic reflection profile showing a fold interference structure similar to the simple kink-band model of Fig. 1. Seismic imaging of interference structure is difficult, but this example clearly shows the anticline over the syncline and a

counter-clockwise interference geometry can be identified that is similar to the theoretical predictions. Furthermore the geometry of the growth strata shows that the sheared kink band formed before the fragmented kink-band. Also note that the beginning of growth on the younger kink-band marks the end of growth on the other (cf. Fig. 3b); the older structure deactivated when the younger activated. This seismic example from the Perdido foldbelt of the Gulf of Mexico (Mount, 1989) is discussed further in the map-view analysis to follow.

INTERFERENCE OF TWO MONOCLINAL FOLDS IN MAP VIEW

In the previous section, we have shown how monoclinal folds generated by different fault-related and multilayer-buckling folding mechanisms interfere with each other in cross section. Now we develop a geometrical map-view model of monocline fold interference. This model does not assume any kind of folding mechanism, but assumes that one fold formed first. A map-view model is useful because in many cases map-scale interference may be best seen in map-view data. Such maps might be based on geologic, seismic or remote sensing data. We use this model to help interpret and elucidate the data in evaluating the role of interference in several examples.

Simple balanced model of three-dimensional interference of two independent monoclinal folds

We consider two monoclinal folds A and B in otherwise horizontal strata that intersect with a map view angle j, which is zero when the two folds are parallel and the limbs dip in the same direction (Fig. 5). To emphasize the essential simplicity of monoclinal interference and to simplify the mathematical development, we model the monoclines as angular, constant-dip kink bands. The map-view geometry of crossing kink bands looks superficially similar to the cross sectional case (Fig. 1). Once the axial surfaces that bound the two kink bands meet, their projections are continuous but deflected. The four intersection points (h, i, j, k) on a single stratigraphic horizon are connected by the deflected sets of axial surfaces forming a closed polygon. Point h is at the lowest or undeformed elevation and k is at the highest elevation. The stratigraphic horizon within this polygon is oriented differently from within the adjacent kink bands. We assume constant limb widths W_a and W_b and dips δ_a and δ_b within the kink-bands away from the interference.

This model considers that the two kink bands are independent and that A forms before B and is deflected by it. Kink band B cuts through A without change in axial-surface orientation outside the intersection zone; for example B might form on a deeper fault and cut across the entire older structure (cf. Fig. 3b). Away from the interference the axial surfaces of both kink bands bisect bedding and conserve layer thickness.

The horizontal displacements due to dip-slip folding (X_a, X_b) away from the interference are given by:

$$X_a = 2W_a \sin^2(\delta_a/2) \tag{1}$$

$$X_b = 2W_b \sin^2(\delta_b/2) \tag{2}$$

The orientation α in map view of the traces of the axial surfaces on the stratigraphic horizon connecting the pairs of points j–h and k–i is given by

$$\alpha = \arctan[X_a \sin\phi/(W_b + X_a \cos\phi)] \tag{3}$$

The orientation β of the traces of the axial surfaces on the stratigraphic horizon connecting the pairs points j–k and h–i is given by

$$\beta = \arctan[X_b \sin\phi/(W_a + X_b \cos\phi)] \tag{4}$$

The present location of the points h, i, j and k, assuming that h is at the origin of a Cartesian coordinate system, is the following:

$$h[0, 0, 0] \tag{5}$$

$$i[W_a/\tan(\phi - \beta), W_a, W_a \tan\delta_a] \tag{6}$$

$$j[-X_a/\tan\alpha, -X_a, W_b \tan\delta_b] \tag{7}$$

$$k[-(X_a/\tan\alpha) + (W_a/\tan(\phi - \beta)), W_a - X_a, W_a \tan\delta_a + W_b \tan\delta_b] \tag{8}$$

Therefore; the dip θ and strike g of the plane containing the points h, i, j, and k are given by

$$\theta = \frac{C}{\sqrt{A^2 + B^2 + C^2}} \tag{9}$$

$$\gamma = \pi/2 - \arctan(-A/B) \tag{10}$$

Where,

$$A = W_a W_b \tan\delta_b + X_a W_a \tan\delta_b \tag{11}$$

$$B = -[W_a W_b \tan\delta_b/\tan(\phi - \beta) + W_a X_a \tan\delta_a/\tan\alpha] \tag{12}$$

$$C = -W_a X_a/\tan(\phi - \beta) + W_a X_a \tan\alpha \tag{13}$$

The calculations of the deflection of the axial surface traces (α, β) and dip and strike (θ, γ) of the plane which contains the intersection points (h,i,j,k) help us to evaluate and produce simplified models of potential interference structures in map view.

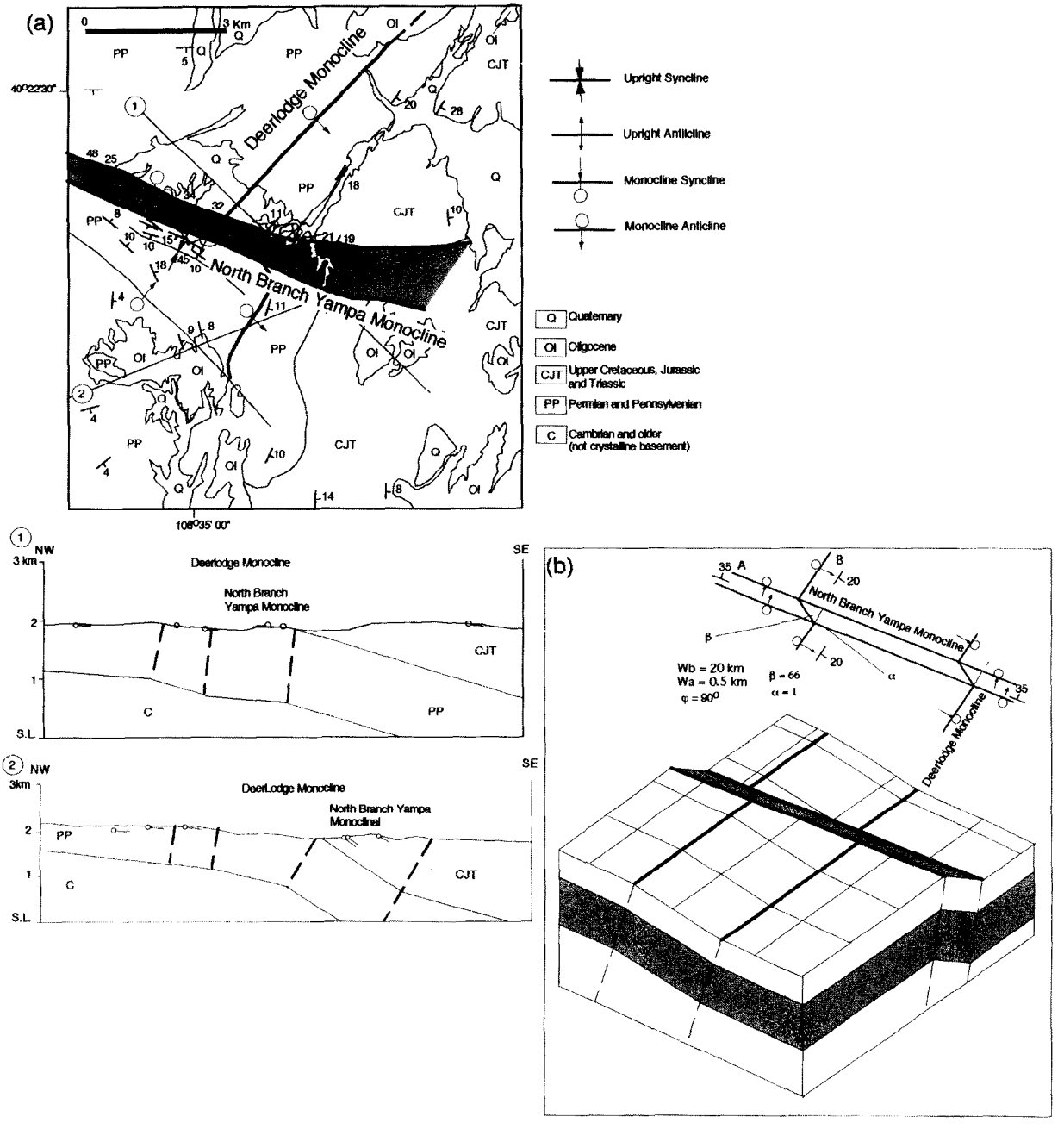

Fig. 8. (a) Modified geologic map of the Indian Water Canyon interference structure, Utah (Hansen *et al.*, 1983). Two cross sections, constructed using the kink method, show the interaction between the North Yampa monocline and the Deerlodge monocline in a vertical plane. We have not interpreted any structure in the Precambrian basement, for lack of constraints. (b) Three dimensional and map view models which illustrate the interference geometry.

EXAMPLES

Teepee interference structure

The Teepee structure is located in the Dinosaur National Monument, Colorado and Utah. This structure is interpreted to be the result of the interaction of two monoclinal folds that face each other (Fig. 6a, b). The Mitten Park monocline trends northeast–southwest and the Ruple Point–Red Rock Anticline trends southeast–northwest (Fig. 7a). As seen in Fig. 6 and documented by mapping of Cook (1978) and Hansen and Rowley (1980a,b) these monoclines show substantial curvature in cross section, whereas the Teepee structure itself, which is the interference fold, is a very tight hinged anticline. Cook (1978) reports that the Weber Sandstone is thickened across the folds (up to 40% thicker), this may in part reflect complex flexural-slip folding processes in the cross-bedded sandstones. These monoclines have been interpreted as caused by faulting in the Uinta Mountain Group, although there is little subsurface control to constrain the geometry of the fault at depth (Cook, 1978; Hansen and Rowley, 1980a,b; Hansen, 1986).

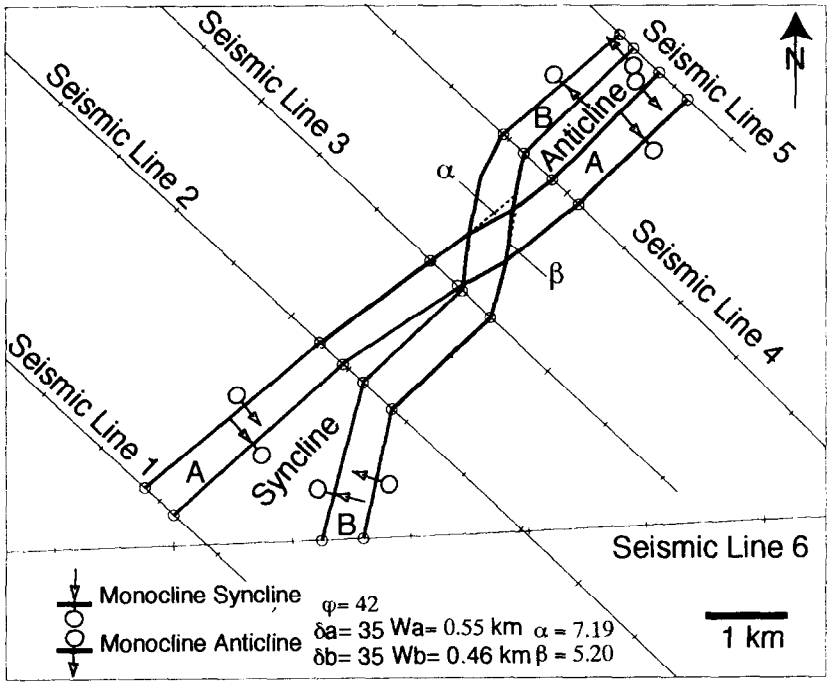

Fig. 9. Axial-surface map of the Perdido fold belt interference structure, offshore Texas, generated by the vertical projection of axial surfaces from a horizon containing the interference anticline. The map-view interference model is used to interpret the information gap between seismic lines 3 and 4.

In order to illustrate the interference between the Mitten Park and Ruple Point–Red Rock monoclinal folds, we approximate the rounded hinges as being defined by a bisecting axial surface. This assumption helps us to visualize the interference geometry and approximates the geometry of the structure. The traces of these axial surfaces are shown in map view (Fig. 7), based on the geologic maps of Hansen and Rowley (1980a,b) and Hansen (1977a,b). The simplified cross section also makes use of this same axial-surface approximation. These maps and cross sections illustrate the interference between the two monoclines in the cover above the Uinta Mountain Group (Proterozoic) (Fig. 7a). Because we are more interested in showing the interference between the monoclinal folds in the cover, we simply continue the monoclines downward into the Uinta Mountain Group, for lack of data. Faulting of the Uinta Mountain Group–Paleozoic contact is assumed in the interpretations of Hansen (1977b), Cook (1978), Hansen and Rowley (1980a,b), Hansen (1986), Brown and Evans (1995) and Brown (1996). The monoclinal folds interfere with each other to form an anticline-over-syncline, clockwise interference structure when viewed from the west (Fig. 7b).

Using the model, we determined the deflection angles (α, β) of the axial surfaces due to the interference. The Mitten Park monocline dips roughly 75° and its limb width in map view is approximately 1270 m, the Ruple Point–Red Rock anticline dips 45° and its limb width is approximately 400 m, and these monoclines interfere at about 35°. Based on these observations β is about 20° and α is 4.6°. These values are close to the geologic map observations. Figure 7(b) shows a three-dimensional model of the Teepee interference structure. We do not have maps on specific stratigraphic horizons, but the interference geometry seems qualitatively similar.

Indian Water Canyon interference structure

The Indian Water Canyon structure is located 40 km southeast of the Teepee structure. It is an interesting example to consider because it appears to result from a close to 90° intersection of the North Yampa and the Deerlodge monoclines. The North Yampa monocline strikes northwest–southeast and the Deerlodge monocline strikes northeast–southwest (Fig. 8a). Both monoclines are curved in cross section (Rowley *et al.*, 1979). Similarly to the folds involved in the Teepee interference structure, they have been interpreted to be related to reverse faulting in the Precambrian basement. Although, there is little subsurface control to constrain the geometry of the fault at depth.

Two cross sections based on a kink approximation of the map by Rowley *et al.* (1979) are presented to show the intersection of the monoclines in a vertical plane (Fig. 8a), although it is difficult to view clearly a 90° monocline interference in cross section. We have not interpreted any kind of structure in the Cambrian and older basement for lack of data.

We have calculated the deflection angles (α, β) of the axial surfaces. The interference angle is 90°. The geologic map shows that the North Branch Yampa monocline

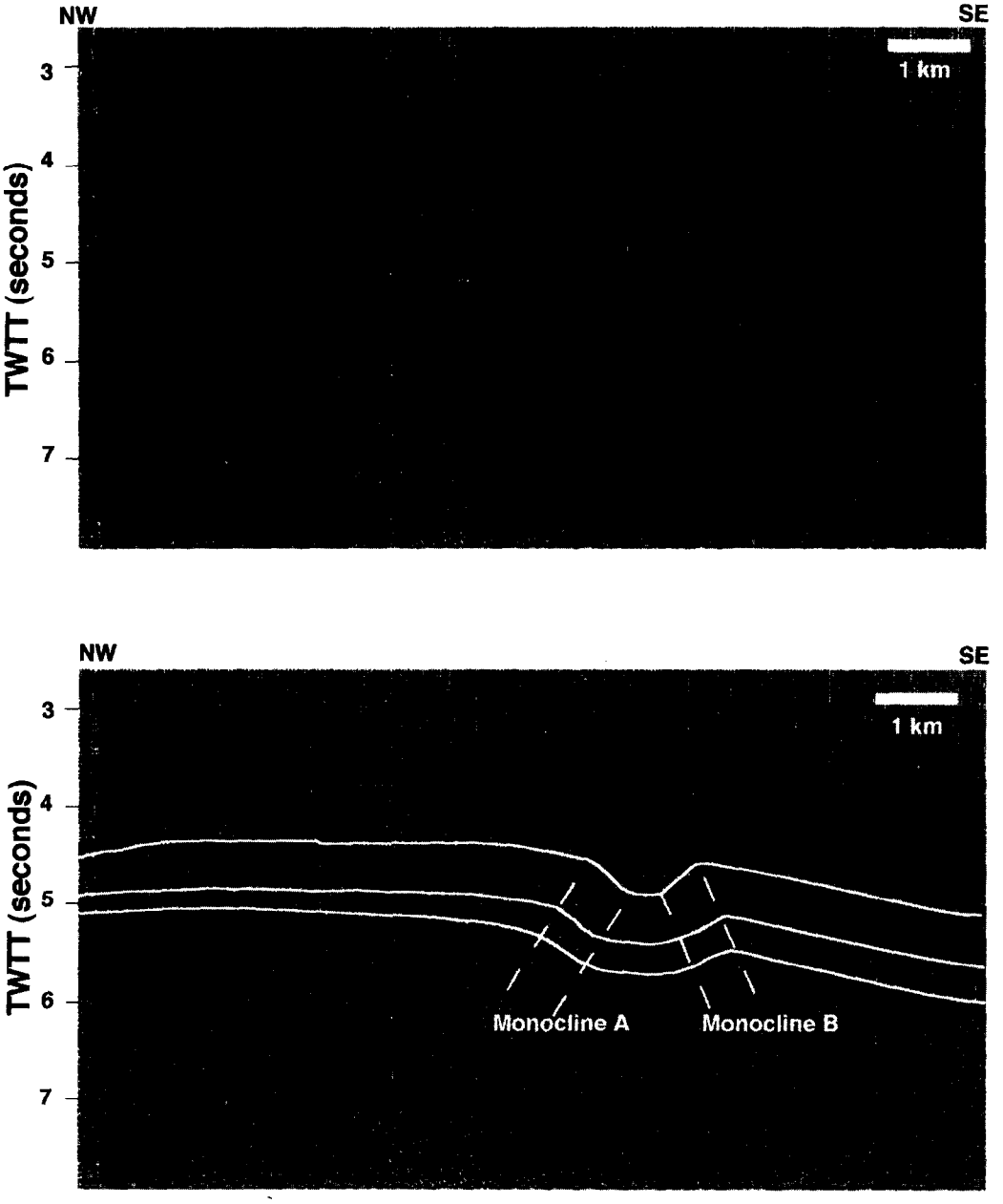

Fig. 10. Seismic reflection profile 2 that illustrates the kink bands (A and B) before interfering with each other. Seismic lines provided by Texaco.

dips 35° and its limb width in map view is approximately 500 m. The Deerlodge monocline dips 20° and its limb width is approximately 20 km. Therefore, β is calculated to be 66° and α is calculated 1°, which are in reasonable agreement with the geologic map derived values of α and β. Figure 8(b) shows a three-dimensional model of the Indian Water Canyon interference structure.

Perdido fold belt interference structure

The interference structure image in seismic section (Fig. 4) is located in the deep-water Perdido fold belt, in the northwest Gulf of Mexico, offshore Texas. Mount (1989) and Trudgill *et al.* (1995a,b) consider this fold belt to have formed in response to gravity sliding over a decollement within the Jurassic salt. Figure 9 is a vertical projection axial surface map of the interference structure using the method of Shaw *et al.* (1994). The map is based on six widely-separated seismic profiles, and it indicates that interference occurs between a pair of conjugate monoclinal folds. Figures 10 and 11 show representative seismic sections in time over the structure. Mount (1989) interprets this structure in cross section as a counter-clockwise, anticline-over-syncline interference structure.

To the south, in seismic line 2 (Fig. 10), we observe two facing monoclines, A and B, separated by a narrow syncline. These two monoclines are the limbs of two much larger anticlines that are interpreted as fault-

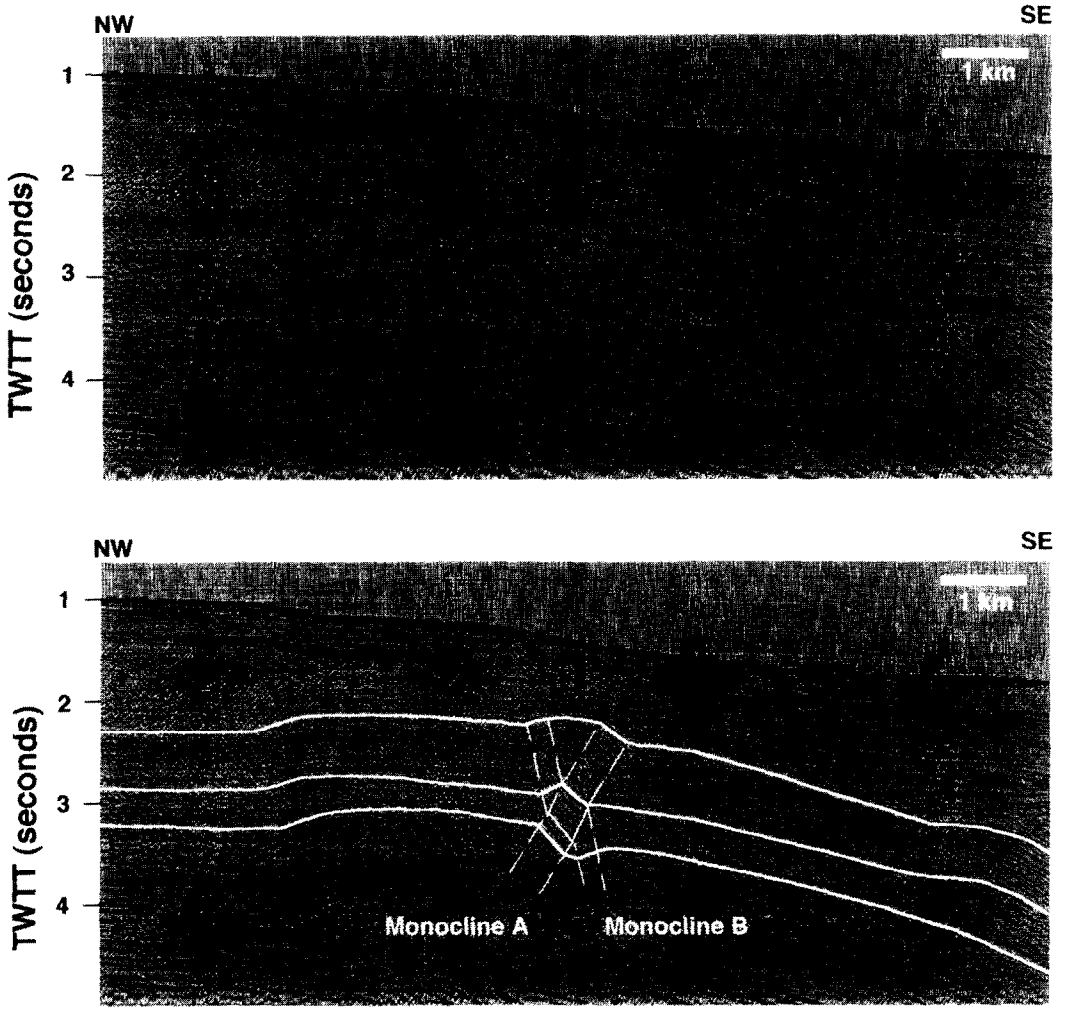

Fig. 11. Seismic reflection profile 4 that images the interference of two kink bands (A and B) in the Perdido fold belt, offshore Texas, Gulf of Mexico. This interference generates a counter-clockwise anticline over syncline interference structure. This is similar to the model depicted in Fig. 1(b). See Fig. 4 for a more detailed view. Seismic line provided by Texaco.

related folds (Mount, 1989 see also Mount *et al.*, 1990), although their specific origin is not important for the interference analysis. Northeast of the intersection of the monoclines (line 4, Fig. 11) an anticline exists at the level of the mapped horizon with the syncline still present at a deeper level. The map-view analysis indicates that the interference actually occurs in the area between seismic lines 3 and 4.

Seismic coverage of the interference zone is not available, but the map-view model can be used to interpret this information gap. We have estimated that the interference angle ϕ is about 42°. The monocline *A* is 550 m wide and dips 35° SE and the monocline *B* is 460 m wide and dips 35° NW. Based on these observations, we obtained the deflection angles (α and β) of 7° and 5°, respectively. The monocline A cuts across B with little deflection, in good agreement with the prediction of α. In contrast, B has a much more irregular strike and its map view geometry is not very well defined by the widely spaced seismic profiles. Thus, the map view geometry is computed from the model and the small computed deflection β is incorporated in the axial surface map (Fig. 9).

Santa Barbara Channel interference structure

This interference structure is located in the Santa Barbara Channel, offshore southern California. A vertical projection axial surface map of this structure is combined with structure contour maps on two important horizons in this basin: the unconformity defined by the onlapping of Pliocene and younger strata and the top Miocene (Fig. 12). The maps were developed using a dense grid consisted of high quality seismic lines. Previously, Ogle *et al.* (1987) developed a map on the top Monterey formation based on well data.

The monoclinal fold interaction occurs between the Oak Ridge and Western Deep folds. These monoclines are interpreted to have been generated by faults at different crustal levels. The Oak Ridge trend is related to a ramp which steps up at around 16 km depth in the crust (Shaw and Suppe, 1994; Shaw *et al.*, 1996). This

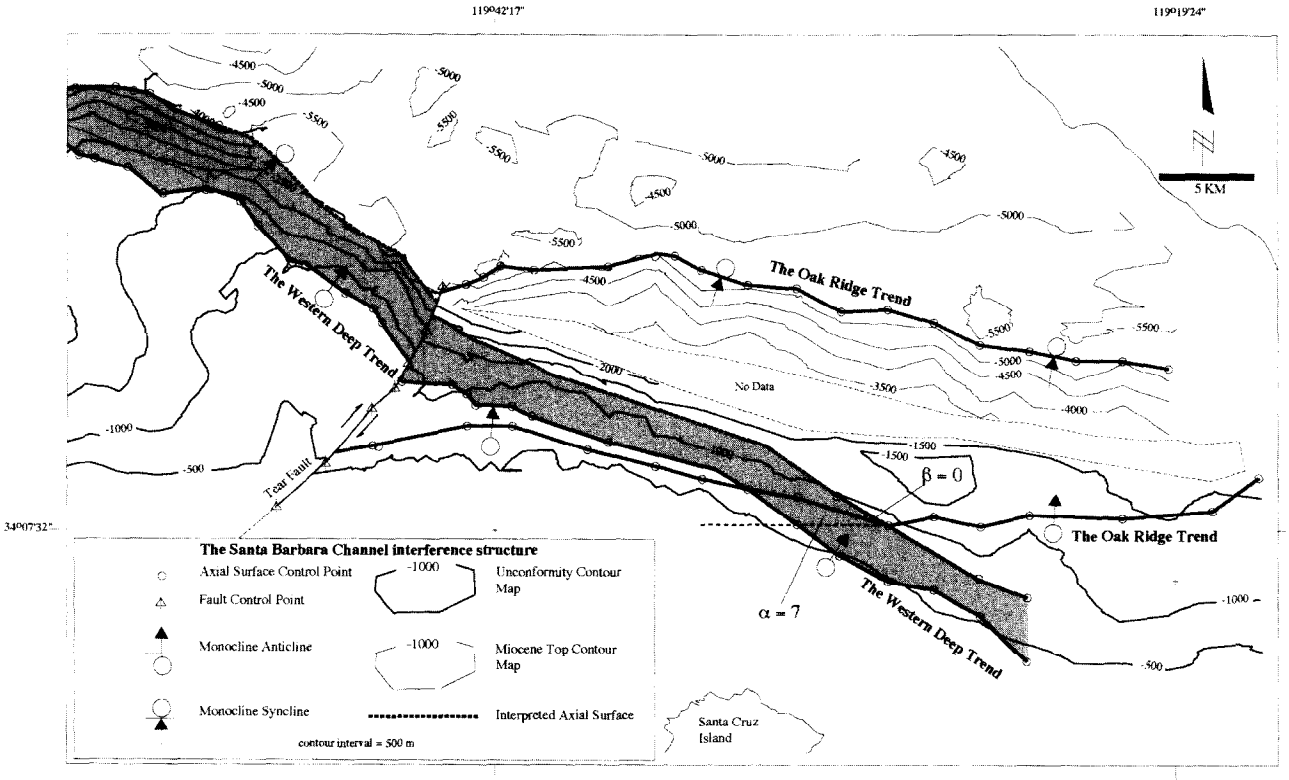

Fig. 12. A combination of contour and vertical projection axial surface maps illustrates the interaction between the Oak Ridge (A, A') and the Western Deep (B, B') monoclinal trends in the Santa Barbara Channel, southern California. The two monoclines intersect quite obliquely. The contour maps represent the top Miocene (thinner lines) and the unconformity defined by onlapping Pliocene and younger strata. The faults generating these monoclines develop at different level in the crust. The Oak Ridge monocline is a back limb related to a south-vergent thrust fault which steps up at about 16 km (Shaw and Suppe, 1994). The Western Deep monocline is a front limb related to a north-vergent fault which flattens at about 4 km (Novoa *et al.*, 1995). The Oak Ridge monocline terminates westward at a major tear fault which is well imaged in seismic profiles, whereas the Western Deep monocline appears to cut across this tear with no major deflection.

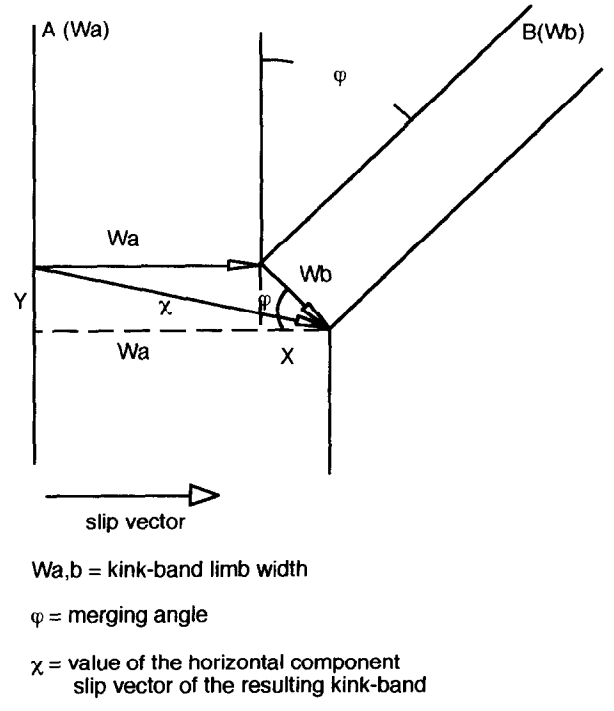

Fig. 13. Simple model of merging kink bands showing the vector sum of the horizontal slip components of kink bands (in this case assumed to be perpendicular to kink bands A and B).

monoclinal syncline terminates abruptly at a tear fault, south of the city of Santa Barbara (Novoa, 1997 see also Novoa *et al.*, 1995). The Western Deep fold is the front limb of a structure which has grown over a north vergent fault at about 4 km depth (Novoa, 1997 see also Novoa *et al.*, 1995).

The Oak Ridge trend is approximately 11 km wide and dips approximately 25° N. The Western Deep trend is approximately 2.4 km wide and dips 15° N. We estimate from the axial surface map that the map view interference angle is about 30° so the deflection angle α is calculated to be 9° and β is close to zero. This result agrees with the mapping in that no clear deflection of axial surfaces is recognized.

MERGING OF MONOCLINAL FOLDS IN MAP VIEW

Monocline merging in map view is another process where two monoclinal folds come together, in this case forming a single monocline. It is important to distinguish merging from the interference discussed above. The merging process could be explained by the merging of two faults at depth, if we assume that the folds were

formed by some kind of fault-related folding mechanism.

To simplify the problem, let us suppose that two kink bands merge in map-view. Then, if the slip vectors in map view of both kink bands are known, we can determine the slip vector horizontal component of the new monocline (Fig. 13). In this simple example the horizontal component of the slip vectors are assumed to be perpendicular to the vertical projection axial surfaces. Then the value of the horizontal component slip vector of the single kink band is given by:

$$L = \sqrt{[W_b \sin \phi]^2 + [W_a + W_b \cos \phi]^2} \qquad (14)$$

Examples of this kind of interaction can be observed in the Colorado Plateau. Figure 14 shows two monoclines merging southward to form the East Kaibab monocline (Maxson, 1967; Reches, 1978). Two simple cross sections show the monoclinal folds, approximated as kink bands. This monocline is 240 km long and develops over a 60–70° average dip reverse faults with minor low angle thrusts (Reches, 1978; Huntoon, 1993).

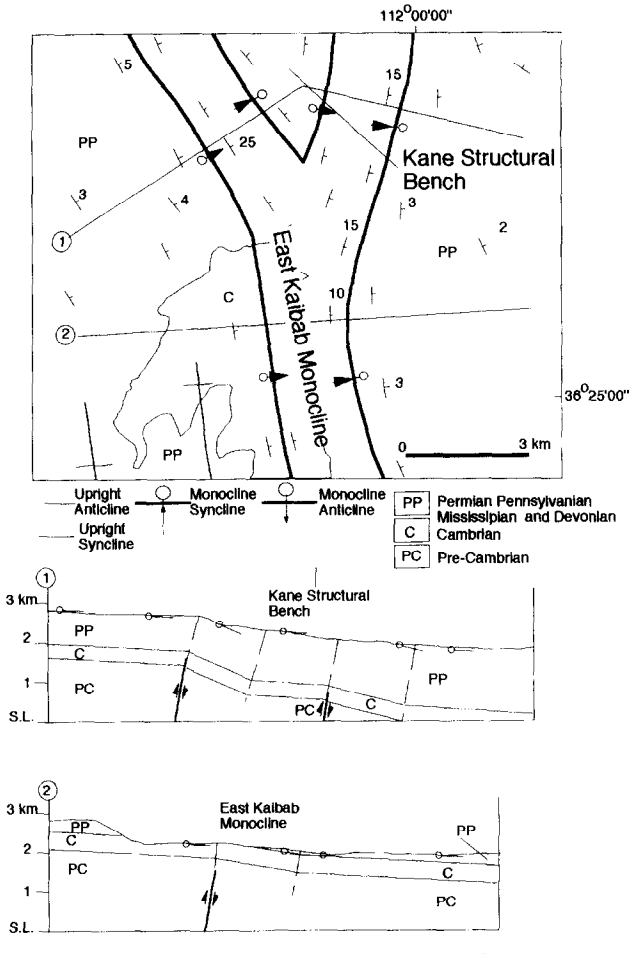

Fig. 14. Geologic map of the east Kaibab monocline area, Grand Canyon, Arizona (Maxson, 1967). Two cross sections illustrate the merging of two kink bands into the east Kaibab monocline.

CONCLUSIONS

Monoclinal folds commonly cross and merge at multiple scales. The structures generated by these processes may be difficult to identify at map scale because they usually are too complex to image or decipher in cross section from reflection seismic profiles and surface geology data. However, because interference in map view may be more easily recognized, we develop a simple model of interference of independent monoclinal kink bands in map view, which does not depend on the folding mechanism, in order to help interpret and evaluate the shapes of potential simple interference structures. Once the kink bands meet, their axial surfaces are continous but deflected in both cross section and map view. This model yields the calculation of the deflection of the axial surface projections the dip and strike of the plane that contains the intersection points.

We have presented five simple, map-scale examples of monoclinal fold interference from the Colorado Plateau, the Perdido foldbelt of the Gulf of Mexico and the Santa Barbara Channel. In four out of five cases, the examples were in reasonable agreement with the theoretical geometric model. In the one exception, from the Perdido foldbelt, the geometry of one of the monoclines in map view is not very well constrained by the available seismic data, althoug

Acknowledgements—Financial support for this research was provided by the following institutions: NEHERP and INTEVEP. We are very grateful to Texaco and Exxon for supplying the seismic lines. In addition, we are grateful for beneficial reviews by Eric Erslev, Joe Gregson, Gary Huftile, Scot Kruger, Don Medwedeff, Ze'ev Reches, Judi Chester and James Evans.

REFERENCES

Alvarez-Marron, J. (1995) Three-dimensional geometry and interference of fault-bend folds: examples from the Ponga unit, Variscan belt NW Spain. *Journal of Structural Geology* **17**, 549–560.

Apotria, T. G., Snedden, W. T., Spang J. H. and Wiltschko, D. V. (1992) Kinematic models of deformation at an oblique ramp. In: *Thrust Tectonics* (edited by McClay, K. R.) Chapman and Hall, London, pp. 141–154.

Brown, C. M. (1996) Structural analysis of the Mitten Park reverse fault and related deformation in Dinosaur National Monument, northwestern Colorado and northeastern Utah: M. S. Thesis, Utah State University, 112pp.

Brown, C. M. and Evans, J. P. (1995) Kinematics of footwall deformation of the Mitten Park fault-fold structure. *Geological Society of America Abstracts with Programs* **27**(4), 4.

Cook, R. A. (1978) A relationship between strike-slip faults and the process of drape folding of layered rocks. In: *Laramide folding associated with basement block faulting in the western United States* (edited by Matthews V.). Geological Society of America Memoir **151**, 197–214.

Erslev, E. A. (1991) Trishear fault propagation folding. *Geology* **19**, 617–620.

Faill, R. T. (1969) Kink band structures in the Valley and Ridge province, central Pennsylvania. *Bulletin of the Geological Society of America* **80**, 2539–2550.

Faill, R. T. (1973) Kink-band folding, Valley and Ridge province, Pennsylvania. *Bulletin of the Geological Society of America* **84**, 1289–1314.

Hansen, W. R. (1977a) *Geologic Map of the Jones Hole Quadrangle,*

Uintah County, Utah and Moffat County, Colorado. U.S. Geological Survey, geologic quadrangle map GQ-1401.

Hansen, W. R. (1977b) *Geologic Map of the Canyon of Lodore South Quadrangle, Moffat County, Colorado.* U.S. Geological Survey, geologic quadrangle map GQ-1403.

Hansen, W. R. and Rowley, P. D. (1980a) *Geologic Map of the Stuntz Reservoir Quadrangle, Utah—Colorado.* U.S. Geological Survey, geologic quadrangle map GQ-1530.

Hansen, W. R. and Rowley, P. D. (1980b) *Geologic Map of the Hells Canyon Quadrangle, Moffat County, Colorado.* U.S. Geological Survey, geologic quadrangle map GQ-1536.

Hansen, W. R., Rowley, P. D. and Carrara, P. E. (1983) *Geologic Map of Dinosaur National Monument and Vicinity, Utah Colorado.* U.S. Geological Survey map I-1407.

Hansen, W. R. (1986) History of faulting in the eastern Uinta mountains, Colorado and Utah. In: *New interpretations of northwest Colorado geology*, eds Stone, D. S. and Johnson, K. S. Rocky Mountain Association of Geologists, 5–17.

Hardy, S. and Ford, M. (1997) Numerical modelling of trishear fault-propagation folding. *Tectonics* **16**, 841–858.

Hardy, S. and Poblet, J. (1994) Geometric and numerical model of progressive limb rotation in detachment folds. *Geology* **22**, 371–374.

Honea, E. and Johnson, A. M. (1976) A theory of concentric, kink and sinusoidal folding and of monoclinal flexuring of compressible, elastic multilayers. IV. Development of sinusoidal and kink folds in multilayers confined by rigid boundaries. *Tectonophysics* **30**, 197–239.

Huntoon, P. W. (1993) Influence of inherited Precambrian basement structure on the localization and form of Laramide monoclines, Grand Canyon, Arizona. In: *Laramide Basement deformation in the Rocky Mountain foreland of the western United States*, eds Schmidt, C. J., Chase, R. B. and Erslev E. *Geological Society of America Special Paper* **280**, 243–256.

Jamison, W. R. (1987) Geometric analysis of fold development in overthrust terranes. *Journal of Structural Geology* **9**, 207–219.

Julivert, M. and Marcos, A. (1973) Superimposed folding under flexural conditions in the Cantabrian zone (Hercynian Cordillera. Northwest Spain). *American Journal of Science* **273**, 353–375.

Lamerson, P. R. (1982) The fossil basin area and its relationship to the Absaroka thrust fault system. In: *Geologic Studies of the Cordilleran Thrust Belt*, ed. Powers, R. B. Rocky Mountain Association of Geologists, 279–340.

Maxson, J. H. (1967) *Preliminary Geologic Map of the Grand Canyon and vicinity, Arizona.* Grand Canyon Natural History Association.

Medwedeff, D. A. (1992) Geometry and kinematics of an active laterally-propagating wedge thrust, Wheeler Ridge, California. In: *Structural Geology of Fold and Thrust Belts* (edited by Mitra, S. and Fisher, G.). John Hopkins University Press, Maryland, 3–28.

Medwedeff, D. A. and Suppe, J. (1997) Multibend fault-bend folding. *Journal of Structural Geology* **19**, 279–292.

Mitra, S. (1990) Fault-propagation folds; geometry, kinematic evolution, and hydrocarbon traps. *Bulletin of the American Association of Petroleum Geologists* **74**, 921–945.

Mount, V. S. (1989) *State of stress in California and a seismic structural analysis of the Perdido Fold Belt, Northwest Gulf of Mexico.* Ph.D. Thesis, Princeton University.

Mount, V. S., Suppe, J. and Hook, S. C. (1990) A forward modeling strategy for balancing cross sections. *Bulletin of the American Association of Petroleum Geologists* **74**, 521–531.

Narr, W. and Suppe, J. (1994) Kinematics of basement-involved compressive structures. *American Journal of Science* **294**, 802–860.

Novoa, E. (1997) *Two and three dimensional analysis of structural trends in the Santa Barbara Channel, California, USA.* Ph.D. Thesis, Princeton University.

Novoa, E. Suppe, J., Mueller, K. and Shaw, J. (1995) Axial surface mapping of active folds in the Santa Barbara Channel. In: *1995 Thrust Ramps and Detachment Faults in the Western Transverse Ranges SCEC workshop* Abs., 19.

Ogle, B. A., Wallis, W. S., Heck, R. G. and Edwards, E. B. (1987) Petroleum geology of the Monterrey formation in the offshore Santa Maria/Santa Barbara areas. In: *Cenozoic basin development of coastal California*, eds Ingersoll, R. V. and Ernst, W. G. Prentice-Hall, Inc., Englewood Cliffs, 382–406.

Paterson, M. S. and Weiss, L. E. (1966) Experimental deformation and folding in phyllite. *Bulletin of the Geologic Society of America* **77**, 343–374.

Reches, Z. (1978) Development of monoclines: Part I. Structure of the Palisades Creek branch of the East Kaibab monocline, Grand Canyon, Arizona. In: *Laramide folding associated with basement block faulting in the western United States*, ed. Matthews, V. *Geological Society of America Memoir* **151**, 235–271.

Rowley, P. D., Dyni, J. R., Hansen, W. R. and Pipiringos, G. N. (1979) *Geologic map of the Indian Water Canyon quadrangle, Moffat County, Colorado.* U.S. Geological Survey, geologic quadrangle map GQ-1516.

Shaw, J. H. and Suppe, J. (1994) Active faulting and growth folding in the eastern Santa Barbara Channel, California. *Bulletin of the Geological Society of America* **106**, 607–626.

Shaw, J. H., Suppe, J. and Hook, S. C. (1994) Structural trend analysis by axial surface mapping. *Bulletin of the American Association of Petroleum Geologists* **78**, 700–721.

Shaw, J. H., Suppe, J. and Hook, S. C. (1996) Structural trend analysis by axial surface mapping: Reply. *Bulletin of the American Association of Petroleum Geologists* **80**, 780–787.

Stewart, S. A. (1993) Fold interference structures in thrust systems. *Tectonophysics* **225**, 449–456.

Stewart, K. G. and Alvarez, W. (1991) Mobile-hinge kinking in layered rock sand models. *Journal of Structural Geology* **13**, 243–259.

Suppe, J. (1983) Geometry and kinematics of fault-bend folding. *American Journal of Science* **283**, 684–721.

Suppe, J. (1985) *Principles of Structural Geology.* Prentice-Hall, Inc., Englewood Cliffs, N.J.

Suppe, J. and Medwedeff, D. A. (1990) Geometry and kinematics of fault-propagation folding. *Ecolgae geologica Helvetica* **83**, 409–454.

Suppe, J., Chou, G. T. and Hook, S. C. (1992) Rates of folding and faulting determined from growth strata. In: *Thrust Tectonics*, ed. McClay, K. R. Chapman and Hall, London, 105–122.

Trudgill, B. D., Fiduk, J. C., Rowan, M. G., Weimer, P., Gale, P. E., Korn, B. E., Phair, R. L., Gafford, W. T., Dischinger, J. B., Roberts, G. R. and Henage, L. F. (1995a) The geological evolution and petroleum potential of the deep water Perdido fold belt, Alaminos canyon, northwestern deep gulf of Mexico. *Gulf Coast Association of Geological Societies Transactions* **45**, 573–579.

Trudgill, B. D., Rowan, M. G., Weimer, P., Fiduk, J. C., Gale, P. E., Korn, B. E., Phair, R. L., Gafford, W. T., Dischinger J. B., Roberts, G. R. and Henage L. F. (1995b) The structural geometry and evolution of the salt-related Perdido fold belt, Alaminos canyon, northwestern deep gulf of Mexico: Gulf Coast Section, Society of Economic Petrologists and Mineralogists Foundation 16th Annual Research Conference, Houston, 275–284.

Weiss, L. E. (1968) Flexural slip folding of foliated model materials. *Geological Survey of Canada* Paper 68-52, 91–106.

Wickham, J. (1995) Fault displacement-gradient folds and the structure at Lost Hills California (U.S.A.). *Journal of Structural Geology* **17**, 1293–1302.

Xiao, H. B. and Suppe, J. (1992) Origin of rollover. *Bulletin of the American Association of Petroleum Geologists* **76**, 509–529.